Hindawi
Adsorption Science & Technology
Volume 2023, Article ID 2808794, 15 pages
https://doi.org/10.1155/2023/2808794

Research Article

Sulphuric Acid-Modified Coal Fly Ash for the Removal of Rhodamine B Dye from Water Environment: Isotherm, Kinetics, and Thermodynamic Studies

G. Bharath Balji[1] **and P. Senthil Kumar**[2]

[1]*Department of Chemical Engineering, Sri Sivasubramaniya Nadar College of Engineering, Kalavakkam 603110, Tamil Nadu, India*
[2]*Centre for Pollution Control and Environmental Engineering, School of Engineering and Technology, Pondicherry University, Kalapet, Puducherry 605014, India*

Correspondence should be addressed to P. Senthil Kumar; senthilkumarp@pondiuni.ac.in

Received 7 August 2023; Revised 13 September 2023; Accepted 19 October 2023; Published 11 November 2023

Academic Editor: Muhammad Raziq Rahimi Kooh

Among the wide variety of dyes present in the environment, cationic dyes are more toxic and have complex structure. The adsorption process of rhodamine B dye was successfully carried out by sulphuric acid-treated inexpensive modified fly ash (MFA) adsorbent via batch experiments. The nature of the adsorbent was characterized by techniques, namely, Fourier transform infrared spectroscopy (FTIR), scanning electron microscopy (SEM), energy-dispersive X-ray spectroscopy (EDX), X-ray diffraction (XRD), and thermogravimetric analysis (TGA). The maximum removal efficiency of RhB dye was found to be 99.78% by using 0.5 g of adsorbent dosage in 50 mg/L of dye concentration. The SEM images displayed the porous nature of the adsorbent where the EDS analysis displays the elemental compositions present in the adsorbent. XRD pattern shows the crystallinity nature of the adsorbent. Among the batch study parameters, effect of pH plays an important role in the adsorption process. The pH of 4 was found to be an ideal setting for the efficient removal of the dye RhB. The preferable elimination ability was found by keeping the dosage at 5 g/L, contact time 120 min, and dye concentration at 50 mg/L. Adsorption capacity was found to be 36.36 mg/g. This shows the ability of the MFA for the removal of wastewater contaminants. This adsorption process is well suited for the Freundlich isotherm, which displaces the process as a multilayer adsorption. Studies in kinetics and thermodynamics demonstrate that the process was well suited for its exothermic nature and pseudo-second-order. Thermal regeneration studies were carried out, and the adsorbent was effectively recycled and utilized up to four more times with minimal loses in its effectiveness. Therefore, from these obtained results, it is clear that the MFA is an effective adsorbent for the effective removal of dyes from wastewater.

1. Introduction

The primary conditions for promoting healthy living are a tidy habitat and safe drinking water. For household use as well as industrial and agricultural purposes, potable water is a necessity. Due to the increasing global population and industrial advancements, a significant amount of water was utilized by residential, industrial, and agricultural activities daily [1]. Some of the manufacturing sectors that use a lot of water include the paper, printing, plastics, leather, and fabric industries [2]. The dyeing process utilized in fabric, paint, food, and cosmetic industries requires vast amounts of water, and the resulting effluent causes serious water pollution. By nature, dyes are nonbiodegradable, carcinogenic, and hard to eliminate from the aqueous medium because of their resilience towards oxidizing chemicals [3–5]. In general, dyes are toxic molecules with benzene groups, which are particularly hazardous substances with high carcinogenicity and mutagenicity. Moreover, the contamination is disturbing public health as well as the ecosystem because it persists [6].

The most dangerous and mutagenic dyes for both humans and marine life are cationic ones. About 12% of the estimated 7 million tonnes of dyes produced each year are discharged into the environment [7, 8]. One of them is

the rhodamine B (RhB) dye, which comes in both cationic and zwitterionic molecular forms [9]. These dyes have various chemical structures with substituted aromatic groups and are positively charged. They are a type of basic dye that dissolves in water and produces colored ions when dissolved [10]. RhB dye is frequently used in a variety of industries but is most prevalent in the textile, paper, and food industries. When RhB is exposed to the environment, it will affect the eyes, respiratory system, and skin of humans and animals. Medical investigations have demonstrated that drinking water contaminated with RhB produces persistent poisoning as well as neurotoxic and carcinogenic effects [11].

Previous reports have shown that RhB is resistant to natural degradation, reproductive toxicity, and animal neurotoxicity [12]. Adsorption [13], membrane filtration [14], electrocoagulation [15], flocculation [16], electrochemical oxidation [17], biological treatment [18], and coagulation are just a few of the methods in the current trend to purify the wastewater [19]. Adsorption, among the other processes, is a useful method for removing dyes because it has a cheap operational cost and good effectiveness, especially if efficient adsorbents are used [20]. Approximately 600 million tonnes of FA are produced annually by combustion power plants that use coal as fuel. Silica, alumina, calcium, unburned carbons, iron, and alkali metal oxides make up most of its composition, along with heavy metal impurities [21, 22]. Fly ashes are classified as F-type and C-type. Fly ash obtained by burning of bituminous coal is termed to be class F, while class C FA originates from burning of subbituminous coal. The major difference between these two types is that class F has no cementing property, while class C has self-cementing properties. Only 20% of the generated FA was utilized in construction purposes, soil stabilization, and zeolite preparation and mainly used as filler material in polymers. These applications cannot fully utilize the production of FA. So, safety disposal of FA is necessary, because if these FA enter into the environment, it will affect the ecosystem by causing water and soil pollution [23–25]. Currently, a significant proportion of FA is being disposed of in simple stacks, monofils, and ponds [26] which are seriously contaminating the water resources, and these disposal techniques are unfriendly to the environment. Additionally, these methods of disposal are taking up large areas of land, including productive farming [27]. So, fly ash is a serious environmental threat and still presents a substantial problem for appropriate disposal [28]. To avoid the hazardous nature of FA by disposing it, effectual utilization of FA in various fields had been emerged. Fly ash has recently been employed in wastewater treatment to remove toxic pollutants economically [29].

The study's unique feature is the use of plentiful, readily available, and cost-effective modified fly ash (MFA) as an adsorbent for the effective and efficient removal of RhB dye. It is an attempt for using sulphuric acid-activated fly ash as an effective adsorbent for organic pollutant removal. The MFA is an easily disposable material, and the fundamental novelty of the operation was to successfully utilize the waste material as an effective adsorbent. As a result, we decided to get rid of it by employing it as a filler material in firecrackers.

This experiment is an attempt to examine the feasibility of modified fly ash (MFA) for the effectual elimination of RhB via batch experiments. Among the various activating agents, sulphuric acid is widely used as an agent for the synthesis of activated carbon. Understanding various activation process parameters is crucial to achieving the desired porosity of carbon for a particular usage. The chemical activation by sulphuric acid enhances the pore development and increases the carbon content in the adsorbent [30]. The batch studies like influences of pH, shaking time, dye concentrations, and dose rate on RhB removal have been evaluated. Adsorption isotherm, thermodynamics, and kinetics studies were also performed and fitted with their respective models. Regeneration studies were conducted as well to determine whether the used adsorbent could be reused.

2. Experimental Studies

2.1. Adsorbent and Chemicals Utilized in This Experiment. For this experimental study, class F fly ash was obtained from the Tuticorin power plant. The main reason for using class F fly ash is that it has only a small amount of cementing properties. So, it cannot be majorly used in the construction industry. All the chemicals used in this analysis are annular class. The rhodamine B dye of $C_{28}H_{31}ClN_2O_3$ 99% purity with analytical reagent (AR) grade was purchased from Sigma-Aldrich Solutions Pvt. Ltd., India, and it was used. The structure of RhB dye is presented in Figure 1. For the chemical activation of fly ash, sulphuric acid (H_2SO_4, 99%, Sigma-Aldrich Solutions Pvt. Ltd., India) was used. 0.1 N of NaOH (97%, Sisco Research Lab Private Limited, India) and 0.1 N of HCl (37.0%, Merck Life Science Pvt. Ltd., India) were used for pH alteration. The stock solution was created by diluting 0.1 g of RhB in 100 mL of water to create synthetic dye wastewater with a 1000 ppm concentration. From the stock solution, the required dye concentration can be made by successive serial dilution.

2.2. Activation and Evaluation of the Adsorbent. The obtained class F fly ash was thoroughly cleaned with double-distilled water repeatedly to get rid of any remaining organic material and then dried in a hot-air oven for 1 day. The uneven particles in the fly ash were grinded using mortar and pestle, and then, it was sieved by using the sieve analysis to get a 40 mm particle size. After acquiring the desired particle size, it was chemically activated using sulphuric acid in a ratio of 1 : 2. After that, the FA was washed several times using double-distilled water to bring back the pH level to neutral. It was then dried for six hours at 120°C in a forced-air circulating oven before being kept in an airtight vessel. After the activation, modified fly ash was characterized by several characterization techniques to examine its applicability and effectiveness. The surface morphology of the MFA was evaluated by EVO18 (Carl Zeiss) scanning electron microscope (SEM). The magnification range was varied between 1000x and 5000x with a 20 kV acceleration voltage. The elemental composition of the adsorbent was analyzed using energy-dispersive X-ray spectrophotometer (Quantax 200 with X Flash 6130). In EDX,

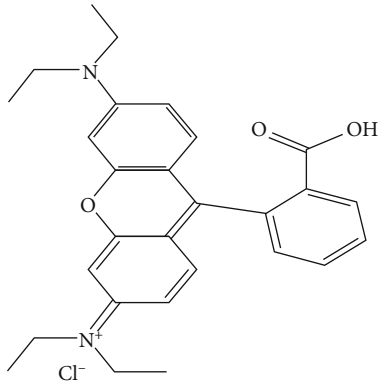

Rhodamine B

Figure 1: Structure of RhB dye.

the composition of the elements can be obtained with the concentration of the available elements. The nature of the adsorbent was evaluated by using D8 advanced X-ray diffractometer (XRD). The varying concentration of rhodamine B was measured by using Jasco-630 UV spectrophotometer. The thermal stability of the MFA was measured by using TGA-DSC with the scanning range of 10°C per minute from 40°C to 1000°C. The functional groups present in the modified FA surface were evaluated by Perkin Elmer e L1600300 Fourier transform infrared spectrometer (FTIR).

2.3. Batch Adsorption Experiments. The study of isotherm and adsorption kinetics will provide the basic knowledge required for designing and operating the instruments in the sewage treatment plant. At 554 nm wavelength, RhB dye was determined using UV spectrophotometer. The batch experiments were executed to evaluate the behaviour of rhodamine B dye on modified fly ash (MFA). The moisture content in the MFA was removed by keeping it in an oven for 3 hours at 110°C. A concentration range of 50 mg/L to 250 mg/L of RhB dye solution was mixed with the desired amount of MFA. Then, it was thoroughly shaken at 150 rpm for extended periods of time at 303 K in a shaker. The concentration of the remaining solution was then examined by UV spectrophotometer after it had been filtered using the Whatman filter paper.

The impact on batch study parameters like pH [3–8] and dose rate (0.1 g-0.8 g), the effect of initial concentration (50 mg/L–250 mg/L), the effect of contact time (15 min-180 min), and the effect of temperature (303 K-318 K) were evaluated. 0.1 N each of HCl and NaOH was used to modify the pH of the mixture.

The sorption experiment was tripled to get consistent results. Freundlich and Langmuir's evaluations were performed to determine the type and capacity of adsorption. To assess the controlling mechanism of this process, kinetic models are used. Since the adsorption process was temperature-dependent, thermodynamic studies were conducted by changing the temperature. The thermodynamic parameters will primarily be used to assess whether this process is possible and spontaneous.

3. Results and Discussion

3.1. Surface Assessment. Using a scanning electron microscope (SEM), the morphology and nature of the modified fly ash (MFA) surface were examined. Before the activation, the surface of the adsorbent was soft and had less pores. Once it was activated with sulphuric acid, the surface becomes rough and had more pores compared with the raw FA. In Figure 2(a), in raw FA, there were no visible pores found on the adsorbent surface. Afterward, scabrous clumps and nonspecific uneven pores are found on the surface of the MFA in Figure 2(b). These active sites will be responsible for the trapping of pollutants. Figure 2(c) displays the trapped RhB molecules in the active site region, and it confirms its effectual nature. The removal of Alizarin Red dye using chemically activated avocado seed powder follows the same pattern, where the adsorbent was chemically activated by using sulphuric acid to enhance its adsorptive properties [31].

3.2. EDS Analysis. Figures 3(a)–3(c) and Table 1 show the EDS stretches of the raw FA and modified fly ash. From Table 1, it is clear that FA and MFA consist of C, O, Na, Mg, Al, Si, S, Ca, Fe, and Ti before and after the adsorption of rhodamine B dye. Out of these elements, carbon and oxygen present in the highest quality. Comparing the before and after activation of FA, the amount of carbon content was increased in the MFA and rhodamine B dye-loaded MFA. The increase of carbon content in MFA is mainly due to the activation by sulphuric acid. Adsorption of RhB dye was confirmed by the increase in the carbon content in rhodamine B dye-loaded MFA. Titanium, iron, sodium, magnesium, sulphur, and potassium along with calcium are present in only the trace amount. Rather than the carbon and oxygen, the amount of silica and aluminium is high because these two are the majority constituents of FA. Due to the presence of dust and dirt, the amount of silica content was increased. Additionally, the sample's insulating properties at the time of analysis may be the cause of the increase in aluminium content. Weight percentage of Mg, Al, and Ca elements was reduced after sulphuric acid activation. This was because these elements will be present in metal oxide form in FA. While activating the FA with sulphuric acid, these metal oxides will be converted to metal sulphates and washed away by distilled water to get neutral pH for MFA.

3.3. XRD Analysis. The morphological changes on the surface of the adsorbent can be evaluated by X-ray diffraction (XRD). The results of the XRD for the FA and MFA are shown in Figure 4. The findings show that the fly ash has more peaks at different angles than the modified fly ash. Amorphous nature and more pores are present in the MFA, due to the evidence of smaller peaks [32]. Due to the sulphuric acid activation, the surface area of the MFA has been raised. The MFA sample has more intensity peaks when compared with the fly ash sample. The major phases of the FA and MFA include quartz and mullite whereas the slight peaks include hematite and magnetite [33].

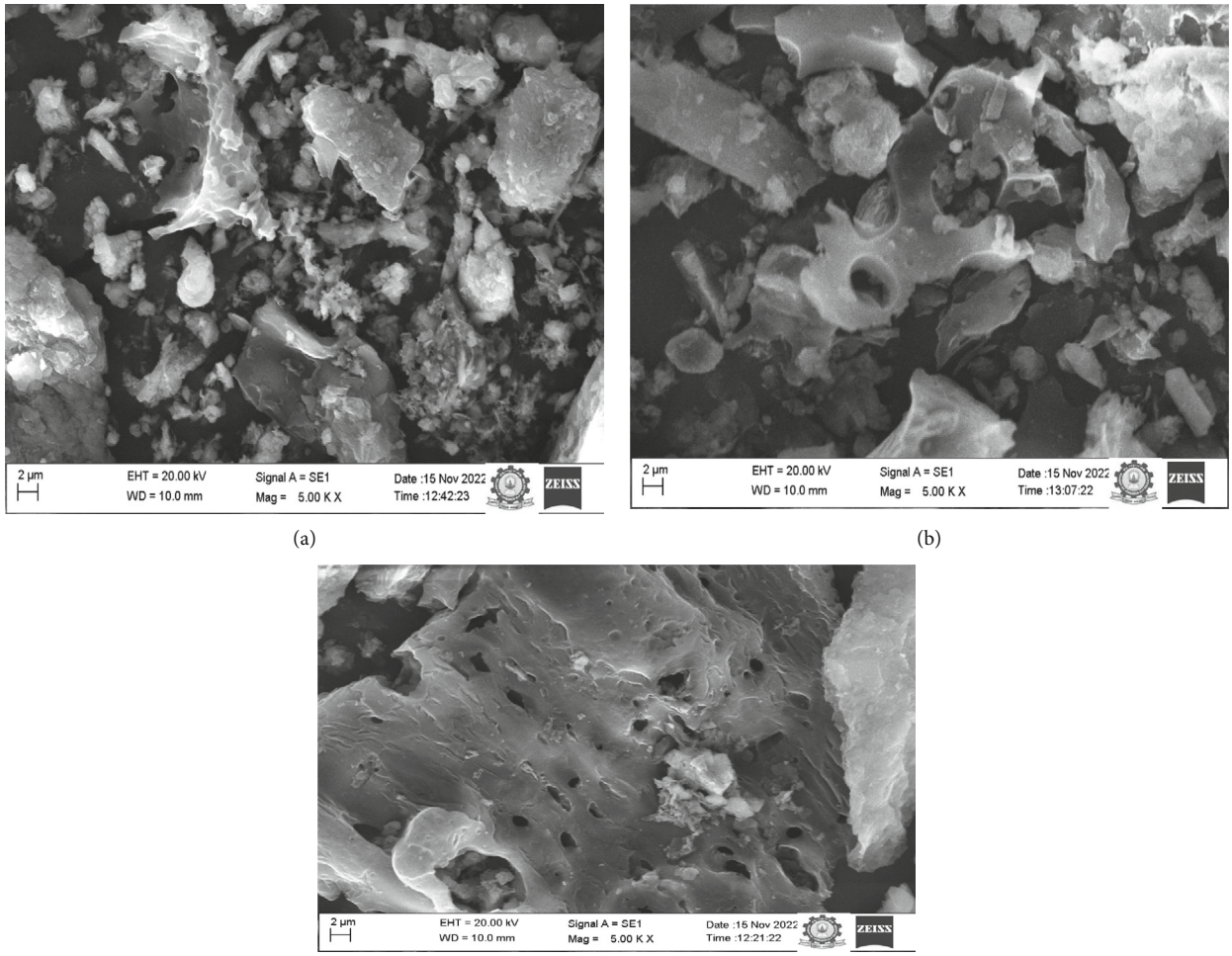

Figure 2: (a) Raw coal fly ash. (b) Modified fly ash (before adsorption). (c) Modified fly ash (after adsorption).

3.4. FTIR Evaluation. Fourier transform infrared spectroscopy is a predominant technique to evaluate the elements on the modified fly ash surface, which enhances the process. The FTIR stretches for the adsorption studies are displayed in Figure 5. The MFA's peak at 1053 and 1060 indicates that silica, the primary substance in FA, is present. The presence of iron oxide components in the FA was displayed by the peaks at 580 and 585 in both evaluations. Stretching between 3200 and 3730 for both before and after adsorption indicates the existence of O-H groups in the MFA adsorbent. A narrow peak shift from 2190 to 2145 indicated the existence of (C≡C stretching) alkyne group and (N=C=N stretching) carbodiimide. A narrow peak in 1975 indicates the presence of the allene group (C=C=C stretching) [34].

3.5. Thermogravimetric Analysis (TGA). Thermogravimetric analysis (TGA) shows an outstanding impact of temperature over the MFA's structure. The reaction between the sulphuric acid and the elements present in the FA will result in the destruction and removal of its amorphous nature. From Figure 6, it is observed that the weight loss occurred in three different stages. From increasing the temperature from 0 to 100°C, only 2.5% of the weight was lost. The moisture content in the MFA is responsible for this loss. Sample weight loss of up to 14% was caused at the temperature range of 100 to 450°C. This major loss was caused by the evaporation or breakdown of physiochemically trapped water. Weight loss from 450 to 1000 is due to the burning of the remaining carbon [35].

3.6. Impact of Shaking Time. One of the key factors used to assess the effectiveness of the adsorbent in the removal of the adsorbate is the effect of the contact time of MFA on rhodamine B dye. The rate of the rhodamine B (RhB) dye removal was evaluated by varying the agitation time from 15 min to 180 min and thereby maintaining the other parameters as same as pH 4, dye concentration 50 mg/L, dose rate 0.5 g, and temperature 30°C, and the results are graphically represented in Figure 7. For this process, the shaking time was maintained at 220 rpm to enhance the rate of the adsorption process. From the figure, it is observed that there is a noticeable increase up to 60 min, where the rate of adsorption of dyes by the active sites will be equal to the desorption of the dye molecules from the already bonded sites, and it results in an equilibrium state. Once the equilibrium state is attained, there will not be any adsorption that

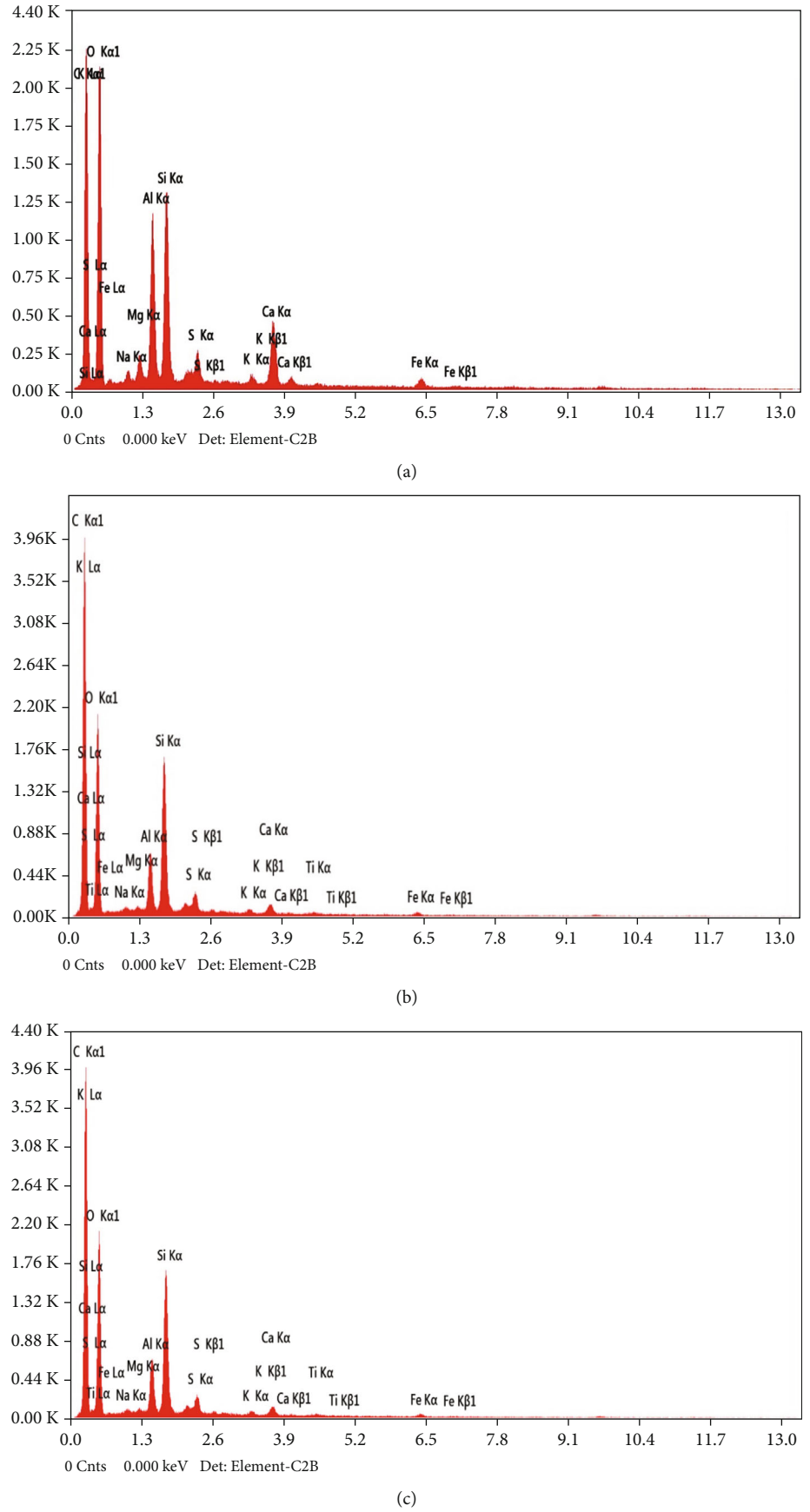

Figure 3: (a) EDS pattern of raw coal FA. (b) EDS pattern of MFA. (c) EDS pattern of MFA (RhB loaded).

Table 1: EDS compositions.

Elements	Weight percentage		
	Fly ash	MFA	MFA (RhB dye loaded)
Carbon (C)	45.4	58.6	64.6
Oxygen (O)	36.1	28.3	26.1
Sodium (Na)	1	0.9	—
Magnesium (Mg)	1.2	0.4	0.3
Aluminium (Al)	4.5	3.3	2.4
Silica (Si)	5.0	5.3	4.5
Sulphur (S)	1.1	1.2	1
Potassium (K)	0.4	0.5	0.2
Calcium (Ca)	3.4	0.5	—
Iron (Fe)	1.5	0.5	0.6
Titanium (Ti)	0.3	0.4	0.3

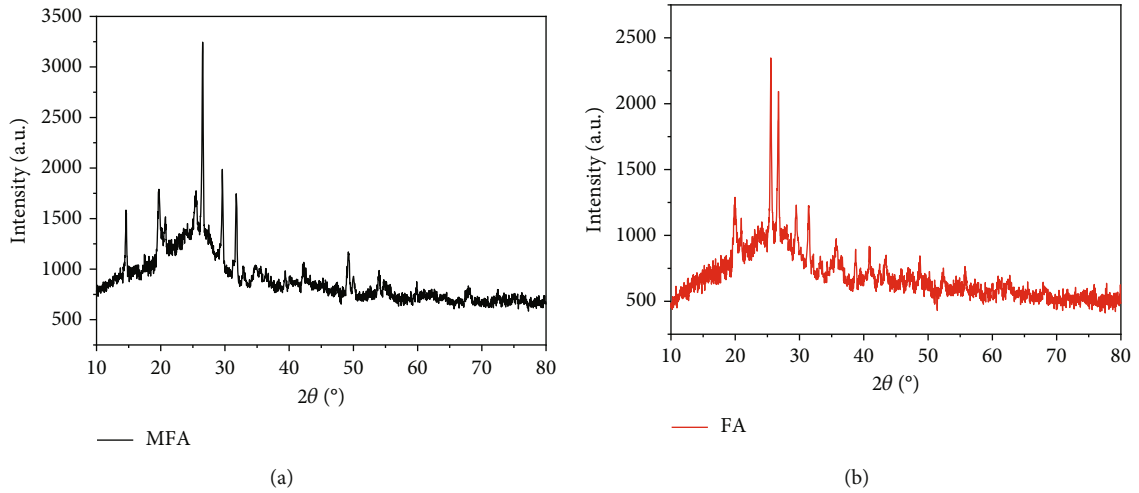

Figure 4: XRD pattern of FA and MFA.

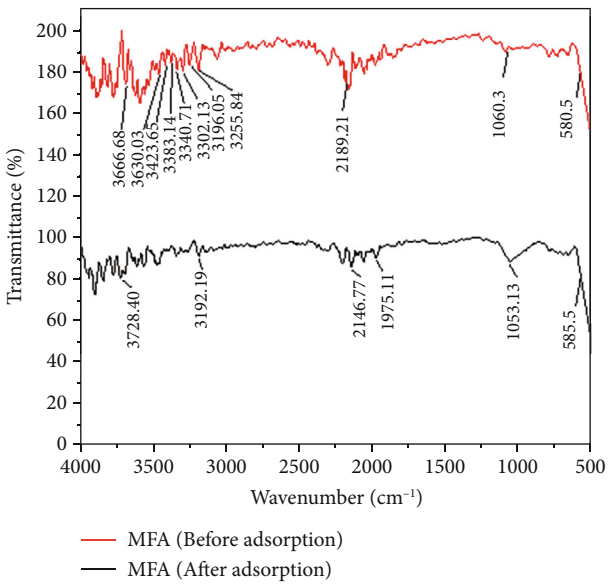

Figure 5: FTIR stretches of modified fly ash (before and after removal).

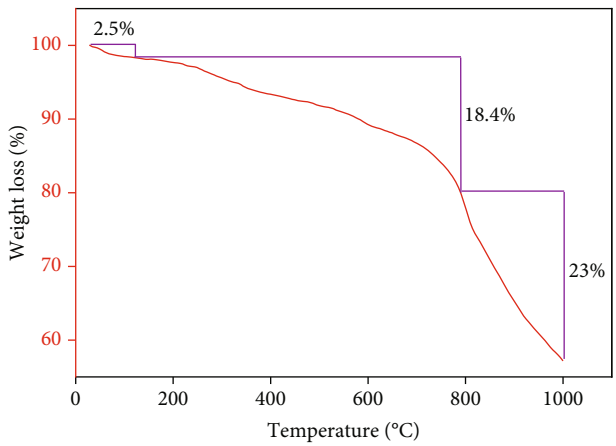

Figure 6: TGA analysis of modified fly ash.

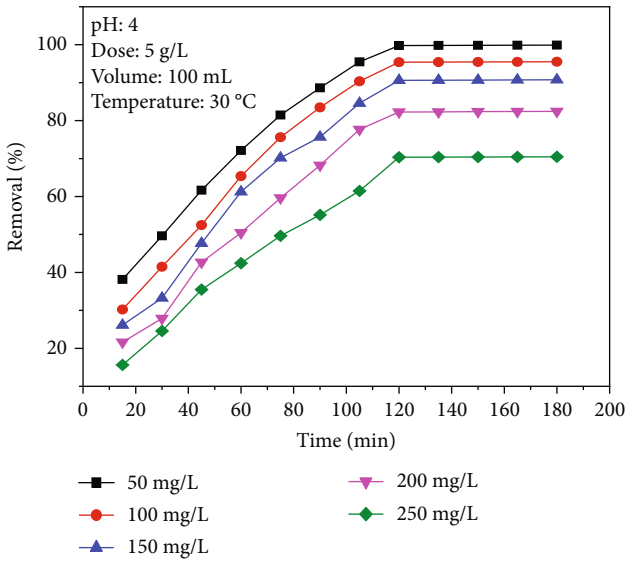

Figure 7: Effect of contact time for the removal of RhB dye.

will take place, because the active sites and the pores are already saturated by the dye molecules. After this period, the remaining active sites will be saturated by three diffusion mechanisms, namely, film, pore, and reactions, that will take place on its surface [36]. Using chemically altered *Volvariella volvacea*, the same general trend of outcome was obtained for the removal of RhB dye [37].

3.7. Impact of MFA Dose Rate. The impact of the MFA dose rate was assessed by altering the MFA dosage from 0.1 to 0.8 g at the same time keeping the other parameters as constant as pH 4, shaking time of 120 min, RhB concentration of 50 mg/L, and temperature of 30°C. With an increase in MFA dosage, rhodamine B dye removal efficiency increased, as shown graphically in Figure 8. A considerable increase from 34% to 99% of dye removal was noticed while increasing the dosage of MFA from 0.1 g to 0.5 g. Once the surface was saturated with dye molecules, further increases in the MFA dosage did not affect the effectiveness of removal. The increased surface area of the MFA and additional potential active sites may be the root cause of the increase in the removal efficiency. After attaining equilibrium, there will not be any further adsorption that will take place, because the dye molecules had already occupied the pores. The removal of RhB dye using a biosorbent from the banana peel produced results that followed a similar pattern [38].

3.8. Impact of pH. To determine the impact of pH, the pH of the solution was varied between 3 and 8. From Figure 9, the adsorption of the dye was reduced while increasing the pH of the solution from 3 to 8. The maximum removal efficiency has occurred at pH 4. The interaction between the rhodamine B dye and the MFA surface was influenced by the ionization states of the different elements held in the surface of the dye molecule and adsorbent. Throughout the process, the quantity of rhodamine B dye adsorbed decreases with increases in pH, and this may be due to the charges on the surface of MFA. At lower pH, it tends to increase the hydronation effect, and it will enhance the adsorption capacity. When the pH of the solution is increased, desorption will take place due to the DE hydronation effect and the adsorption efficiency of rhodamine B will tend to decline. The pH at zero point charge for the MFA was estimated by the drift method, and it is shown in Figure 10. When the pH is higher than the pH_{ZPC}, electrostatic repulsion will happen between the adsorbent and the adsorbate and the removal efficiency will also decrease [35]. Using biomass of cypress/false cypress, the removal of RhB dye produced results that followed an identical trend [39].

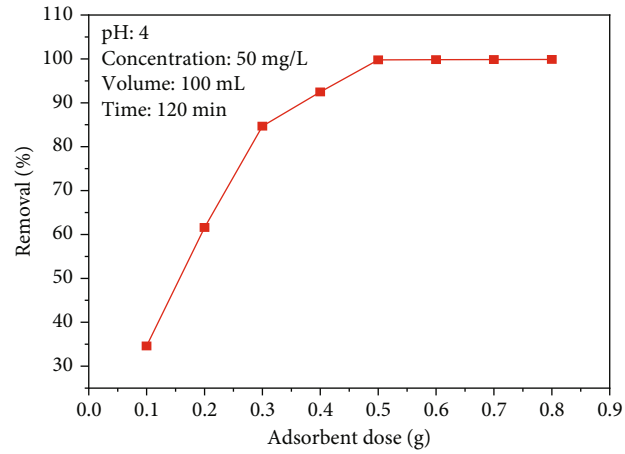

Figure 8: Impact of adsorbent dosage for the removal of RhB dye.

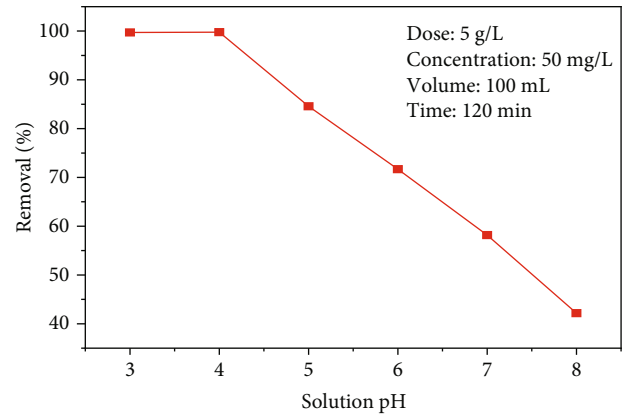

Figure 9: Effect of pH for the removal of RhB dye.

3.9. Impact of Rhodamine B Concentration. The impact of rhodamine B concentration was evaluated by altering the dye concentration from 50 to 250 mg/L. According to the results in Figure 11, the removal efficiency decreases as the initial dye concentration of rhodamine B dye rises. But when raising the concentration of the rhodamine B, the adsorption capacity of the dye keeps on increasing. It is because when the concentration of the adsorbate rises, the driving force also rises [40]. The main reason for more removal at lower concentrations is because of the availableness of binding sites and pores on the modified fly ash (MFA). The decrease in the removal efficiency is due to the unavailability of active sites for the dye molecules to attach to the adsorbent surface.

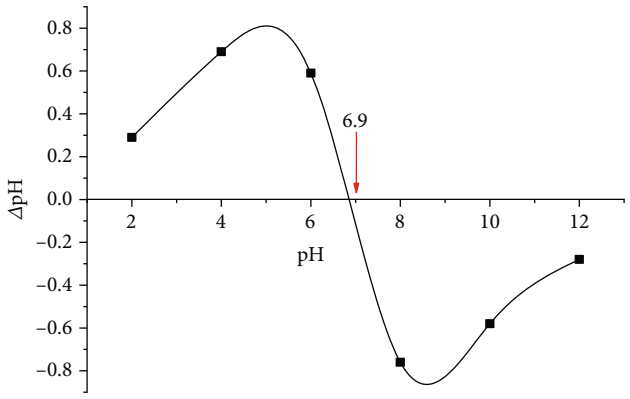

Figure 10: Zero point charge of MFA.

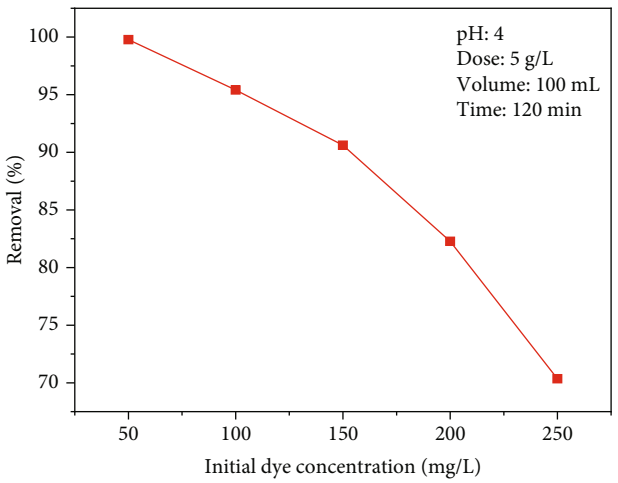

Figure 11: Impact of initial dye concentration for the removal of RhB dye.

The same tendency of result was observed in the effectual removal of rhodamine B dye by using MgO-loaded Fe-Co-Mn nanoparticles [11].

3.10. Impact of Temperature and Thermodynamics. To examine the suitable temperature, the investigations were by altering the temperature ranging from 303 K to 318 K and thereby keeping the other parameters like pH [4], RhB dye concentration (50 mg/L), shaking time (120 min), and dose rate (5 g/L) as constant. From Figure 12, it is noticeable that the increasing temperature will decrease the adsorption efficiency. The weakening of the electrostatic field of attraction may be the main cause of the decreased efficacy of RhB uptake by the MFA at higher temperatures. At higher temperatures, the dye molecules will desorb from the adsorbed active sites. Hence, it is evidenced that the lower temperature will be evident for an enhancement in the adsorption effectiveness of RhB dye by using MFA adsorbent. Using magnetic silica alginite beads (MSAB) as an adsorbent, a similar sequence of outcomes was obtained for the adsorption of RhB dye [41].

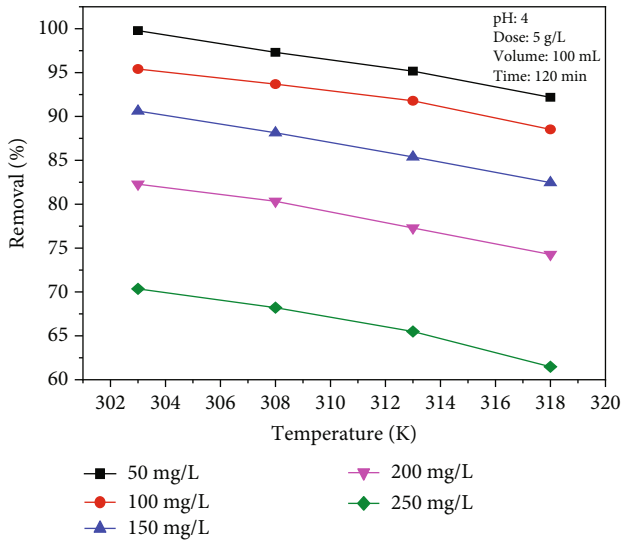

Figure 12: Effect of temperature for the removal of RhB dye.

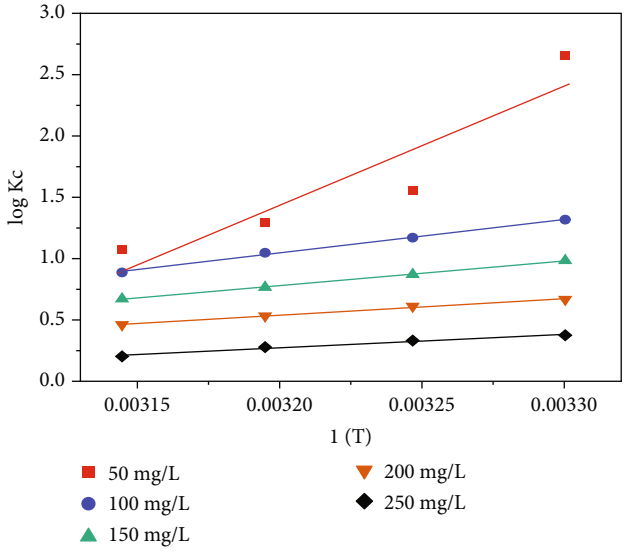

Figure 13: Thermodynamic evaluation.

The main reason for performing the thermodynamic evaluation is to determine the suitable nature and spontaneity of this process. By utilizing Van 't Hoff's equations, the thermodynamic parameters for adsorption studies can be calculated by the following equations:

$$\begin{aligned} \mathrm{Kc} &= \frac{C_{\mathrm{Ae}}}{C_{\mathrm{e}}}, \\ \Delta G^{\circ} &= -\mathrm{RTlnKc}, \\ \Delta G^{\circ} &= \Delta H^{\circ} - T\Delta S^{\circ}, \\ \ln \mathrm{Kc} &= -\frac{\Delta H^{\circ}}{\mathrm{RT}} + \frac{\Delta S^{\circ}}{\mathrm{R}}, \\ \log \mathrm{Kc} &= -\frac{\Delta H^{\circ}}{2.303\,\mathrm{RT}} + \frac{\Delta S^{\circ}}{2.303\,R}. \end{aligned} \tag{1}$$

Table 2: Parameters of thermodynamics.

RhB concentration (mg/L)	ΔH^o (kJ/mol)	ΔS^o (J/mol·K)	ΔG^o (kJ/mol)			
			303 K	308 K	313 K	318 K
50	-80.822	-568.166	-15.409	-9.188	-7.756	-6.522
100	-22.661	-146.954	-7.643	-6.904	-6.278	-5.400
150	-16.714	-108.219	-5.713	-5.136	-4.594	-4.092
200	-11.175	-72.031	-3.867	-3.604	-3.187	-2.803
250	-9.112	-61.921	-2.176	-1.954	-1.667	-1.236

By plotting a graph for $1/T$ vs. log Kc, ΔH^o and ΔS^o values can be determined by using slope and intercept readings from Figure 13. The determined values are listed in Table 2. From the table, it is evident that ΔG^o, ΔH^o, and ΔS^o values belong to negative. ΔG negative value shows the feasibility of the process. The negative value of ΔH^o describes the exothermic nature. The negative value of ΔS^o demonstrates that the adsorption process was enthalpy-driven, with reduced randomness [42].

3.11. Adsorption Isotherms. The effectiveness and the controlling mechanism of the adsorption process can be approximately determined by using isotherm studies. These studies will explain about how the adsorbate molecules at equilibrium conditions interacted with the adsorbent surface. The Langmuir and Freundlich adsorption isotherms were implemented to obtain a proper interactivity between the adsorption and desorption rate of rhodamine B dye onto modified fly ash (MFA). The isotherm model and isotherm data were obtained by plotting a graph between C_e vs. q_e.

The Langmuir adsorption isotherm model is a mathematical model in which the surface of the adsorbent is assumed to be homogeneous, and the adsorbate is assumed to adsorb in a monolayer [43]. The mathematical expression was given as

$$q_e = \frac{q_{max} K_L C_e}{1 + K_L C_e}, \quad (2)$$

where q_e corresponds to the quantity of RhB adsorbed per gram of the MFA at equilibrium (mg^{-1}), K_L is termed to be Langmuir constant (L/mg), C_e is the equilibrium concentration of the RhB (mg/L), and q_{max} is the monolayer adsorption capacity (mg/g).

The Freundlich isotherm is a nonideal, reversible, and multilayer adsorption isotherm model. The Freundlich model explains the heterogeneous surface with varying active sites' energy [44]. The mathematical expression of the Freundlich isotherm was given as

$$q_e = K_F C_e^{1/n}, \quad (3)$$

where K_F ((mg/g) $(L/mg)^{1/n}$) is termed to be Freundlich constant, it will be used to examine the adsorption degree, and $1/n$ represents the heterogeneity factor of adsorption.

Figure 14 and Table 3 show the equilibrium evaluation and the parameters of the isotherm analysis. Based on the R^2 value and the error readings, the best model that suit for this adsorption process was chosen. From Table 3, it is clear that the system follows the Freundlich isotherm because it has a greater R^2 value (0.9812) and lower error value of SSE (8.1) and RMSE (1.643).

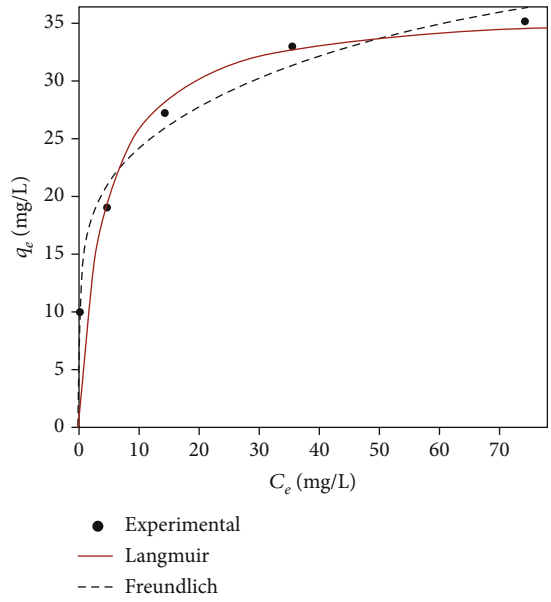

Figure 14: Isotherm evaluation for the removal of RhB by MFA.

Table 3: Adsorption isotherm parameters.

Models	Parameters	Values
Langmuir	K_L (L/mg)	0.2507
	q_{max} (mg/g)	36.36
	R^2	0.8077
	SSE	82.99
	RMSE	5.26
Freundlich	K_F ((mg/g) $(L/mg)^{1/n}$)	15.27
	n	4.956
	R^2	0.9812
	SSE	8.1
	RMSE	1.643

Table 4: Adsorption capacities of already available adsorbents.

Materials	Dyes	Favourable pH	Time (min)	Isotherm model	Maximum adsorption capacity (mg/g)	Ref.
Waste of seeds of *Aleurites moluccanus*	RhB	6	120	Sips	117	[49]
Paper industry waste	RhB	2.4	60	Langmuir	6.711	[46]
Okra waste	RhB	3.5	600	Langmuir	321.50	[50]
Saw dust	RhB	1-11	10	Langmuir	35.7	[47]
Sulphur-doped biochar from tapioca peel waste	RhB	8	120	Langmuir	32.810	[51]
Coffee waste powder	RhB	2	180	Langmuir	5.26	[48]
Artocarpus odoratissimus leaves	RhB	3	30	Langmuir	104.96	[52]
Kaolinite	RhB	7	80	Langmuir	46.08	[53]
Linde-type A zeolite from CFA	Acid red 66	4	10	Freundlich	416.7	[54]
CFA	Methylene blue (MB)	—	—	Langmuir	2.88	[55]
Activated CFA	MB	—	—	Langmuir	37.08	[55]
Bentonite carbon nanotubes	RhB	9	30	Freundlich	142.8	[56]
Sodium dodecyl sulfate-modified Fe_2O_3 (zeolite)	RhB	3	60	Freundlich	89.3	[57]
A coral reef-shaped mesoporous silica material obtained from CFA	MB	9	60	Langmuir	10.86	[58]
Modified fly ash (MFA)	RhB	4	120	Freundlich	36.36	This study

The mathematical expression of SSE and RMSE [45] is given below.

$$\mathrm{SSE} = \sum_{i=1}^{n} (A_i - P_i)^2,$$
$$\mathrm{RMSE} = \sqrt{\sum_{i=1}^{n} \frac{(A_i - P)^2}{n}}. \quad (4)$$

So, in this process, the removal of RhB dye was carried out in a multilayer with a heterogeneous structure. By calculating the number of adsorbates adsorbed on the adsorbents using adsorption isotherms, the saturated adsorption capacity for adsorbates for various adsorbents can be compared. Various adsorbents synthesized from the waste materials and CFA are listed in Table 4. And this table comprises the bibliographic review of adsorbents with their adsorption capacity and the nature of adsorption. While being compared with the adsorption capacities of biomass wastes like paper industry waste [46], saw dust [47], and coffee waste power [48], MFA (this work) displays higher adsorption capacity of 36.36 mg/g. The prepared absorbent was cost-effective and had multilayers for better removal efficiency. Compared with the zeolites prepared from the CFA, this adsorbent was easy to synthesize and it can be regenerated up 4 cycles with minimal loss in its efficiency.

3.12. Adsorption Kinetics. The kinetic models will provide the information about the equilibrium time required to carry out the adsorption process. It is an essential tool for developing an adsorption system. It delivers details regarding the rate of the process and the effectiveness of the material used. Kinetic models, namely, pseudo-first-order (PFO) [59] and pseudo-second-order (PSO) [60] and intraparticle diffusion (IPD) [61], are used in this study to evaluate the adsorption kinetics and mechanism of MFA adsorbent. The nonlinear equations of the kinetic models are listed below.

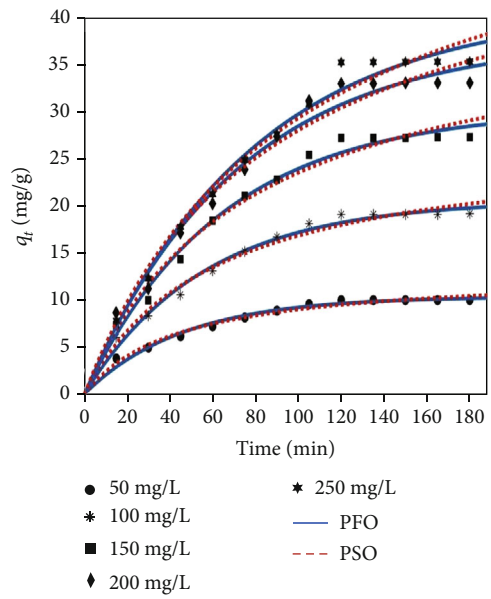

Figure 15: Adsorption kinetics for the elimination of RhB by MFA.

$$q_t = q_e(1 - \exp(-k_1 t)) \quad (\mathrm{PFO}),$$
$$q_t = \frac{q_e^2 k_2 t}{1 + q_e k_2 t} \quad (\mathrm{PSO}), \quad (5)$$
$$q_t = k_p t^{1/2} + C \quad (\mathrm{IPD}),$$

Table 5: Kinetic parameters of MFA for the removal of RhB dye.

Models	Parameters	Values				
		50 mg/L	100 mg/L	150 mg/L	200 mg/L	250 mg/L
PFO	q_e exp (mg/g)	10.12	19.25	27.35	33.11	35.32
	k_1 (min^{-1})	0.02192	0.018	0.01571	0.01401	0.01285
	q_e cal (mg/g)	10.36	20.55	30.19	37.71	41.04
	R^2	0.9742	0.9815	0.9831	0.976	0.984
	SSE	1.368	4.52	9.671	21.68	16.9
	RMSE	0.3699	0.6723	0.9834	1.472	1.3
PSO	k_2 (g/mg·min)	0.00176	0.00061	0.00032	0.00021	0.00017
	q_e cal (mg/g)	12.95	26.94	41.06	52.63	58.28
	R^2	0.9754	0.9736	0.9732	0.9673	0.9781
	SSE	1.301	6.447	15.36	29.52	23.11
	RMSE	0.3606	0.8029	1.239	1.718	1.52
IPD	k_p (mg/(g·$min^{(1/2)}$))	0.6997	1.2039	1.8315	2.3418	2.5686
	C	1.615	6.2437	7.569	7.7712	7.2541
	R^2	0.9298	0.8485	0.857	0.8684	0.8924

where q_t is the concentration of the pollutant adsorbed at equilibrium time (t), q_e is the concentration of the pollutant adsorbed at equilibrium, k_1 is the PFO rate constant, k_2 is the PSO rate constant, and k_p is the IPD rate constant.

By using the kinetic model equations listed above, the kinetic models (Figure 15) and the obtained data are tabulated in Table 5. From the table, it is clear that the correlation coefficient (R^2) of PFO is considerably higher than the PSO model. There was no major difference in the q_e cal and q_e exp values in the PFO model as compared with PSO model. So, it was decided that the adsorption of RhB dye by MFA adsorbent fitted in the PFO model and the nature of adsorption was physisorption. The gradual decrease in the value of rate constant (k) while increasing the concentration of the dye indicates the lower availability of the active sites for the adsorbates to adhere on the adsorbent surface. At higher concentrations, there will be more competition for the RhB dye to attach on the surface of the adsorbent. Diffusion mechanism may be the controlling mechanism of the adsorption process, where intraparticle diffusion (IPD) is a mass transfer phenomenon that occurs at three different stages (Figure 16) that include external diffusion which is the first stage in which the pollutant, namely, the adsorbate, will diffuse through the aqueous film nearer to the adsorbent. Internal diffusion is the second stage, in which the pollutant will be dispersed into the inner region of the pores on the surface of the material.

3.13. Effect of Coions. Common dye wastewater usually contains some specific amount of other existing materials, namely, inorganic salts. For the industrial implementation of modified fly ash (MFA) for adsorption application, the impact of the other coions, namely, organic salts, needs to be evaluated. This study includes some of the inorganic salts, namely, KCl, NaCl, K_2SO_4, and KNO_3, that were used for evaluation. Figure 17 shows that there were negligible impacts on the adsorption effectiveness of RhB dye in the existence of these organic salts. Therefore, modified fly ash has a higher ability, and it can be implemented for real-time wastewater treatment.

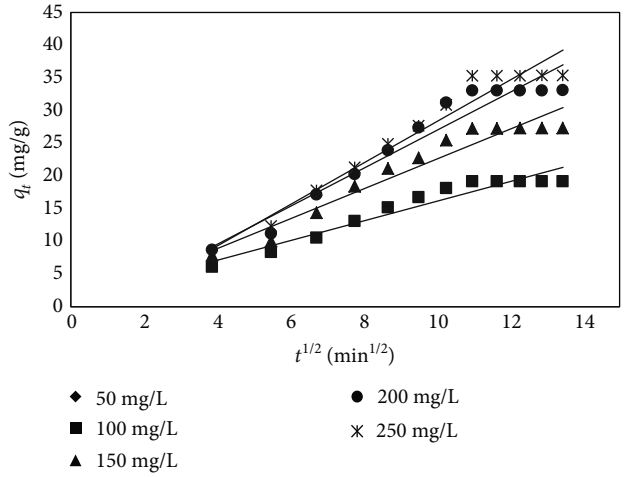

Figure 16: Intraparticle diffusion.

3.14. Regeneration Studies. The process of regeneration is another crucial criterion to examine the efficiency of the material. Before starting the regeneration process, the adsorbate molecules need to be desorbed from the adsorbent with some methods. And the method we used needs not to disintegrate or disturb the structure of the adsorbent. A wide variety of methods are available for desorption and regeneration studies. Modified fly ash is an inorganic material, so it has high thermal stability when compared with other organic adsorbents. The MFA was regenerated using the technique of heating because of its high thermal stability.

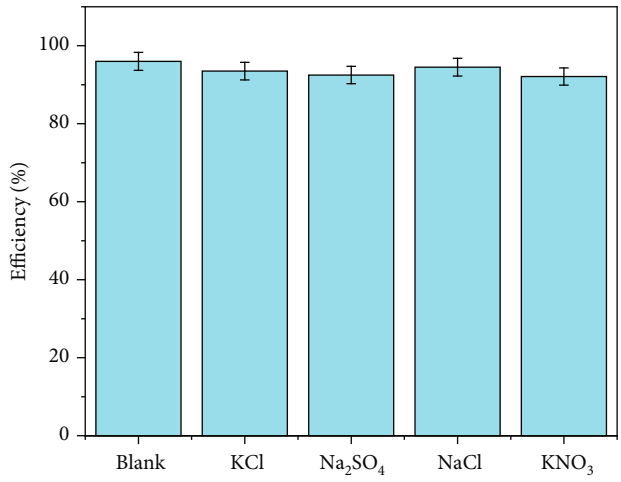

Figure 17: Effect of coions for the removal of RhB dye.

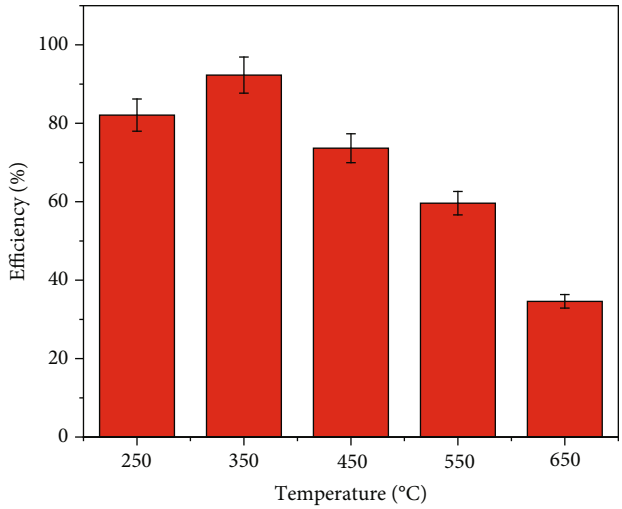

Figure 18: Regeneration studies of MFA.

For the regeneration studies, the adsorbent was saturated by agitating 0.5 g of MFA with 100 mL of a 100 mg/L RhB dye solution for 24 hrs, and then, it was filtered. The filtrate was oven dried at 120°C. The temperature from 250°C, 350°C, 450°C, 550°C, and 650°C was utilized to investigate the adsorption efficiency of the regenerated MFA. Figure 18 displays that 350°C will be the suitable temperature. MFA can also be recycled and reused up to four times with little efficiency loss.

3.15. Adsorption Mechanism. There exist π-π interaction, hydrogen bonding, and electrostatic attraction between the adsorbate RhB and the adsorbent MFA. From the obtained FTIR spectrum results of before and after adsorption, the date revealed the formation of carbodiimide bond between MFA and RhB. The π-π interaction occurred between the unsaturated aromatic ring in the RhB dye and the alkyne system in the MFA. Then, from the observed FTIR, data above 3100 cm^{-1} express the -OH stretching frequency, and this reveals the existence of hydrogen bonding between the adsorbent and the adsorbate [9, 62].

4. Conclusion

The present experiment displays the elimination of rhodamine B (RhB) dye as a synthetic effluent using the modified fly ash (MFA). The characterization experiments like FTIR, TGA, XRD, SEM, and EDS studies were carried out. The XRD results clearly show that once the adsorbent is activated by using the sulphuric acid, its crystallinity nature was reduced and it becomes more amorphous in nature. Among the batch study parameters, effect of pH plays a major impact. The pH of 4 was determined as a suitable state for the effectual removal of RhB. The preferable elimination ability was found by keeping the dosage at 5 g/L, contact time 120 min, and dye concentration at 50 mg/L. This adsorption process is well suited for the Freundlich isotherm, which displaces the process as a multilayer. Studies in kinetics and thermodynamics demonstrate that the process was well suited for its exothermic nature and pseudo-second-order (PSO). According to studies on reusability, the adsorbent can be reused up to four times without significantly losing effectiveness. Based on the results, it is concluded that the activation of fly ash using sulphuric acid enhances the surface area and porous nature of fly ash and thereby promotes the adsorption effects on RhB. For the future prospective, MFA can be applied in a column study for treating a continuous flow of water rather than a batch study. Moreover, the usability of the MFA adsorbent for the treatment of real wastewater can be evaluated. Additionally, the reduction in the chemical oxygen demand (COD) using MFA can be evaluated.

Data Availability

All data generated or analyzed during this study are included in this published article.

Conflicts of Interest

The authors declare that there are no conflicts of interest for this article. No copyediting or translation services were used for the preparation of this manuscript.

Authors' Contributions

G. Bharath Balji was responsible for the investigation and methodology and wrote the original draft. P. Senthil Kumar was responsible for the conceptualization, validation, and supervision.

References

[1] R. Rashid, I. Shafiq, P. Akhter, M. J. Iqbal, and M. Hussain, "A state-of-the-art review on wastewater treatment techniques: the effectiveness of adsorption method," *Environmental Science and Pollution Research*, vol. 28, no. 8, pp. 9050–9066, 2021.

[2] H. Wang, Z. Li, S. Yahyaoui et al., "Effective adsorption of dyes on an activated carbon prepared from carboxymethyl cellulose: experiments, characterization and advanced modelling," *Chemical Engineering Journal*, vol. 417, article 128116, 2021.

[3] M. R. Gadekar and M. M. Ahammed, "Modelling dye removal by adsorption onto water treatment residuals using combined response surface methodology-artificial neural network approach," *Journal of Environmental Management*, vol. 231, pp. 241–248, 2019.

[4] M. K. Uddin and U. Baig, "Synthesis of Co_3O_4 nanoparticles and their performance towards methyl orange dye removal: characterisation, adsorption and response surface methodology," *Journal of Cleaner Production*, vol. 211, pp. 1141–1153, 2019.

[5] A. H. Jawad, A. S. Abdulhameed, and M. S. Mastuli, "Acid-factionalized biomass material for methylene blue dye removal: a comprehensive adsorption and mechanism study," *Journal of Taibah University for Science*, vol. 14, no. 1, pp. 305–313, 2020.

[6] P. Sirajudheen, P. Karthikeyan, S. Vigneshwaran, and S. Meenakshi, "Synthesis and characterization of La(III) supported carboxymethylcellulose- clay composite for toxic dyes removal: evaluation of adsorption kinetics, isotherms and thermodynamics," *International Journal of Biological Macromolecules*, vol. 161, pp. 1117–1126, 2020.

[7] R. Foroutan, R. Mohammadi, J. Razeghi, and B. Ramavandi, "Performance of algal activated carbon/Fe_3O_4 magnetic composite for cationic dyes removal from aqueous solutions," *Algal Research*, vol. 40, p. 101509, 2019.

[8] H. Ma, A. Kong, Y. Ji, B. He, Y. Song, and J. Li, "Ultrahigh adsorption capacities for anionic and cationic dyes from wastewater using only chitosan," *Journal of Cleaner Production*, vol. 214, pp. 89–94, 2019.

[9] U. Jinendra, D. Bilehal, B. M. Nagabhushana, and A. P. Kumar, "Adsorptive removal of rhodamine B dye from aqueous solution by using graphene–based nickel nanocomposite," *Heliyon*, vol. 7, no. 4, p. e06851, 2021.

[10] M. O. Ojemaye and A. I. Okoh, "Multiple nitrogen functionalized magnetic nanoparticles as an efficient adsorbent: synthesis, kinetics, isotherm and thermodynamic studies for the removal of rhodamine B from aqueous solution," *Scientific Reports*, vol. 9, no. 1, p. 9672, 2019.

[11] S. Rahdar, A. Rahdar, M. N. Zafar, S. S. Shafqat, and S. Ahmadi, "Synthesis and characterization of MgO supported Fe-Co-Mn nanoparticles with exceptionally high adsorption capacity for rhodamine B dye," *Journal of Materials Research and Technology*, vol. 8, no. 5, pp. 3800–3810, 2019.

[12] Z. Ren, F. Chen, B. Wang, Z. Song, Z. Zhou, and D. Ren, "Magnetic biochar from alkali-activated rice straw for removal of rhodamine B from aqueous solution," *Environmental Engineering Research*, vol. 25, no. 4, pp. 536–544, 2020.

[13] A. H. Jawad, R. Razuan, J. N. Appaturi, and L. D. Wilson, "Adsorption and mechanism study for methylene blue dye removal with carbonized watermelon (*Citrullus lanatus*) rind prepared via one-step liquid phase H_2SO_4 activation," *Surfaces and Interfaces*, vol. 16, pp. 76–84, 2019.

[14] H. Liu, J. Zhang, M. Lu, L. Liang, H. Zhang, and J. Wei, "Biosynthesis based membrane filtration coupled with iron nanoparticles reduction process in removal of dyes," *Chemical Engineering Journal*, vol. 387, p. 124202, 2020.

[15] S. C. M. Signorelli, J. M. Costa, and A. F. de Almeida Neto, "Electrocoagulation-flotation for orange II dye removal: Kinetics, costs, and process variables effects," *Journal of Environmental Chemical Engineering*, vol. 9, no. 5, article 106157, 2021.

[16] X. Zhao, X. Wang, G. Song, and T. Lou, "Microwave assisted copolymerization of sodium alginate and dimethyl diallyl ammonium chloride as flocculant for dye removal," *International Journal of Biological Macromolecules*, vol. 156, pp. 585–590, 2020.

[17] S. Cotillas, J. Llanos, P. Cañizares et al., "Removal of Procion Red MX-5B dye from wastewater by conductive-diamond electrochemical oxidation," *Electrochimica Acta*, vol. 263, pp. 1–7, 2018.

[18] K. Piaskowski, R. Świderska-Dąbrowska, and P. K. Zarzycki, "Dye removal from water and wastewater using various physical, chemical, and biological processes," *Journal of AOAC International*, vol. 101, no. 5, pp. 1371–1384, 2018.

[19] A. H. Jawad, A. S. Abdulhameed, and M. S. Mastuli, "Mesoporous crosslinked chitosan-activated charcoal composite for the removal of thionine cationic dye: comprehensive adsorption and mechanism study," *Journal of Polymers and the Environment*, vol. 28, no. 3, pp. 1095–1105, 2020.

[20] Z. Li, L. Sellaoui, D. Franco et al., "Adsorption of hazardous dyes on functionalized multiwalled carbon nanotubes in single and binary systems: experimental study and physicochemical interpretation of the adsorption mechanism," *Chemical Engineering Journal*, vol. 389, p. 124467, 2020.

[21] G. Atun, N. Ayar, A. E. Kurtoğlu, and S. Ortaboy, "A comparison of sorptive removal of anthraquinone and azo dyes using fly ash from single and binary solutions," *Journal of Hazardous Materials*, vol. 371, pp. 94–107, 2019.

[22] N. N. Abd Malek, A. H. Jawad, K. Ismail, R. Razuan, and Z. A. Alothman, "Fly ash modified magnetic chitosan-polyvinyl alcohol blend for reactive orange 16 dye removal: adsorption parametric optimization," *International Journal of Biological Macromolecules*, vol. 189, pp. 464–476, 2021.

[23] Z. T. Yao, X. S. Ji, P. K. Sarker et al., "A comprehensive review on the applications of coal fly ash," *Earth-Science Reviews*, vol. 141, pp. 105–121, 2015.

[24] K. Mirković, N. Tošić, and G. Mladenović, "Effect of different types of fly ash on properties of asphalt mixtures," *Advances in Civil Engineering*, vol. 2019, Article ID 8107264, 11 pages, 2019.

[25] P. L. Meyyappan and G. Bharathbalji, "Effect of flyash in enhancing the strength and durability characteristics of foam concrete," *International Journal of Recent Technology and Engineering*, vol. 8, no. 4S2, pp. 60–63, 2019.

[26] J. Zhou, K. Xia, X. Liu, L. Fang, H. Du, and X. Zhang, "Utilization of cationic polymer-modified fly ash for dye wastewater treatment," *Clean Technologies and Environmental Policy*, vol. 23, no. 4, pp. 1273–1282, 2021.

[27] N. Wang, X. Sun, Q. Zhao, Y. Yang, and P. Wang, "Leachability and adverse effects of coal fly ash: a review," *Journal of Hazardous Materials*, vol. 396, p. 122725, 2020.

[28] S. Chakraborty, A. Mukherjee, S. Das, N. R. Maddela, S. Iram, and P. Das, "Study on isotherm, kinetics, and thermodynamics of adsorption of crystal violet dye by calcium oxide modified fly ash," *Environmental Engineering Research*, vol. 26, no. 1, 2021.

[29] W. Astuti, A. Chafidz, E. T. Wahyuni, A. Prasetya, I. M. Bendiyasa, and A. E. Abasaeed, "Methyl violet dye removal

using coal fly ash (CFA) as a dual sites adsorbent," *Journal of Environmental Chemical Engineering*, vol. 7, no. 5, article 103262, 2019.

[30] C. K. Singh, J. N. Sahu, K. K. Mahalik, C. R. Mohanty, B. R. Mohan, and B. C. Meikap, "Studies on the removal of Pb (II) from wastewater by activated carbon developed from Tamarind wood activated with sulphuric acid," *Journal of Hazardous Materials*, vol. 153, no. 1-2, pp. 221–228, 2008.

[31] G. Bharath Balji and P. Senthil Kumar, "Adsorptive removal of Alizarin Red S onto sulfuric acid-modified avocado seeds: kinetics, equilibrium, and thermodynamic studies," *Adsorption Science & Technology*, vol. 2022, Article ID 3137870, 13 pages, 2022.

[32] Z. Hussain, N. Chang, J. Sun et al., "Modification of coal fly ash and its use as low-cost adsorbent for the removal of directive, acid and reactive dyes," *Journal of Hazardous Materials*, vol. 422, p. 126778, 2022.

[33] A. Taufiq, P. Hidayat, and A. Hidayat, "Modified coal fly ash as low cost adsorbent for removal reactive dyes from batik industry," *In MATEC Web of Conferences*, vol. 154, p. 1037, 2018.

[34] V. K. Yadav, G. K. Inwati, D. Ali et al., "Remediation of azure a dye from aqueous solution by using surface-modified coal fly ash extracted ferrospheres by mineral acids and toxicity assessment," *Adsorption Science & Technology*, vol. 2022, Article ID 7012889, 14 pages, 2022.

[35] P. Sirajudheen, P. Karthikeyan, K. Ramkumar, and S. Meenakshi, "Effective removal of organic pollutants by adsorption onto chitosan supported graphene oxide-hydroxyapatite composite: a novel reusable adsorbent," *Journal of Molecular Liquids*, vol. 318, p. 114200, 2020.

[36] I. C. De Sá, P. O. Silva, E. Nossol et al., "Modified dry bean pod waste (*Phaseolus vulgaris*) as a biosorbent for fluorescein removal from aqueous media: batch and fixed bed studies," *Journal of Hazardous Materials*, vol. 424, article 127723, 2022.

[37] Q. Li, X. Tang, Y. Sun et al., "Removal of rhodamine B from wastewater by modified *Volvariella volvacea*: batch and column study," *RSC Advances*, vol. 5, no. 32, pp. 25337–25347, 2015.

[38] S. Singh, N. Parveen, and H. Gupta, "Adsorptive decontamination of rhodamine-B from water using banana peel powder: a biosorbent," *Environmental Technology & Innovation*, vol. 12, pp. 189–195, 2018.

[39] S. Gul, H. Gul, M. Gul et al., "Enhanced adsorption of rhodamine B on biomass of cypress/false cypress (*Chamaecyparis lawsoniana*) fruit: optimization and kinetic study," *Water*, vol. 14, no. 19, p. 2987, 2022.

[40] B. T. Gemici, H. U. Ozel, and H. B. Ozel, "Removal of methylene blue onto forest wastes: adsorption isotherms, kinetics and thermodynamic analysis," *Environmental Technology & Innovation*, vol. 22, article 101501, 2021.

[41] G. J. Joshiba, P. S. Kumar, M. Govarthanan, P. T. Ngueagni, A. F. C. C. Abilarasu, and F. Carolin C, "Investigation of magnetic silica nanocomposite immobilized *Pseudomonas fluorescens* as a biosorbent for the effective sequestration of rhodamine B from aqueous systems," *Environmental Pollution*, vol. 269, article 116173, 2021.

[42] G. B. Balji, A. Surya, P. Govindaraj, and G. M. Ponsakthi, "Utilization of fly ash for the effective removal of hazardous dyes from textile effluent," *Inorganic Chemistry Communications*, vol. 143, article 109708, 2022.

[43] I. Langmuir, "The adsorption of gases on plane surfaces of glass, mica and platinum," *Journal of the American Chemical Society*, vol. 40, no. 9, pp. 1361–1403, 1918.

[44] H. M. F. Freundlich, "Over the adsorption in solution," *The Journal of Physical Chemistry*, vol. 57, no. 385471, pp. 1100–1107, 1906.

[45] O. E. Agwu, J. U. Akpabio, and A. Dosunmu, "Artificial neural network model for predicting drill cuttings settling velocity," *Petroleum*, vol. 6, no. 4, pp. 340–352, 2020.

[46] A. Thakur and H. Kaur, "Response surface optimization of rhodamine B dye removal using paper industry waste as adsorbent," *International Journal of Industrial Chemistry*, vol. 8, no. 2, pp. 175–186, 2017.

[47] D. T. Nguyen, T. T. Nguyen, H. P. T. Nguyen et al., "Activated carbon with ultrahigh surface area derived from sawdust biowaste for the removal of rhodamine B in water," *Environmental Technology & Innovation*, vol. 24, article 101811, 2021.

[48] K. Shen and M. A. Gondal, "Removal of hazardous rhodamine dye from water by adsorption onto exhausted coffee ground," *Journal of Saudi Chemical Society*, vol. 21, pp. S120–S127, 2017.

[49] D. L. Postai, C. A. Demarchi, F. Zanatta, D. C. C. Melo, and C. A. Rodrigues, "Adsorption of rhodamine B and methylene blue dyes using waste of seeds of *Aleurites moluccana*, a low cost adsorbent," *Alexandria Engineering Journal*, vol. 55, no. 2, pp. 1713–1723, 2016.

[50] O. Üner, Ü. Geçgel, H. Kolancilar, and Y. Bayrak, "Adsorptive removal of rhodamine B with activated carbon obtained from okra wastes," *Chemical Engineering Communications*, vol. 204, no. 7, pp. 772–783, 2017.

[51] S. Vigneshwaran, P. Sirajudheen, P. Karthikeyan, and S. Meenakshi, "Fabrication of sulfur-doped biochar derived from tapioca peel waste with superior adsorption performance for the removal of malachite green and rhodamine B dyes," *Surfaces and Interfaces*, vol. 23, p. 100920, 2021.

[52] N. A. H. Mohamad Zaidi, L. B. Lim, N. Priyantha, and A. Usman, "Artocarpus odoratissimus leaves as an eco-friendly adsorbent for the removal of toxic rhodamine B dye in aqueous solution: equilibrium isotherm, kinetics, thermodynamics and regeneration studies," *Arabian Journal for Science and Engineering*, vol. 43, no. 11, pp. 6011–6020, 2018.

[53] T. A. Khan, S. Dahiya, and I. Ali, "Use of kaolinite as adsorbent: equilibrium, dynamics and thermodynamic studies on the adsorption of rhodamine B from aqueous solution," *Applied Clay Science*, vol. 69, pp. 58–66, 2012.

[54] T. Al-dahri, A. A. AbdulRazak, and S. Rohani, "Preparation and characterization of Linde-type A zeolite (LTA) from coal fly ash by microwave-assisted synthesis method: its application as adsorbent for removal of anionic dyes," *International Journal of Coal Preparation and Utilization*, vol. 42, no. 7, pp. 2064–2077, 2022.

[55] M. El Alouani, S. Alehyen, M. El Achouri, and M. H. Taibi, "Comparative study of the adsorption of micropollutant contained in aqueous phase using coal fly ash and activated coal fly ash: kinetic and isotherm studies," *Chemical Data Collections*, vol. 23, article 100265, 2019.

[56] M. I. Mohammed and S. Baytak, "Synthesis of bentonite–carbon nanotube nanocomposite and its adsorption of rhodamine dye from water," *Arabian Journal for Science and Engineering*, vol. 41, no. 12, pp. 4775–4785, 2016.

[57] A. A. AbdulRazak and S. Rohani, "Sodium dodecyl sulfate-modified Fe_2O_3/molecular sieves for removal of rhodamine B dyes," *Advances in Materials Science and Engineering*, vol. 2018, Article ID 3849867, 10 pages, 2018.

[58] S. Sareen, S. Kaur, V. Mutreja, A. Sharma, S. K. Kansal, and S. K. Mehta, "Coral-reef shaped mesoporous silica obtained from coal fly ash with high adsorption capacity," *Topics in Catalysis*, vol. 65, no. 19-20, pp. 1791–1810, 2022.

[59] S. K. Lagergren, "About the theory of so-called adsorption of soluble substances," *Sven. Vetenskapsakad. Handingarl*, vol. 24, pp. 1–39, 1898.

[60] Y. S. Ho and G. McKay, "Pseudo-second order model for sorption processes," *Process Biochemistry*, vol. 34, no. 5, pp. 451–465, 1999.

[61] W. J. Weber Jr. and J. C. Morris, "Kinetics of adsorption on carbon from solution," *Journal of the Sanitary Engineering Division*, vol. 89, no. 2, pp. 31–59, 1963.

[62] X. Chen, H. Li, W. Liu et al., "Effective removal of methyl orange and rhodamine B from aqueous solution using furfural industrial processing waste: furfural residue as an eco-friendly biosorbent," *Colloids and Surfaces A: Physicochemical and Engineering Aspects*, vol. 583, p. 123976, 2019.